

Quark model calculation of $\eta \rightarrow l^+l^-$ to all orders in the bound-state relative momentum

Bernard Margolis

Physics Department, McGill University, 3600 University Street, Montreal, Quebec, Canada H3A 2T8

John N. Ng

TRIUMF, 4004 Wesbrook Mall, Vancouver, British Columbia, Canada V6T 2A3

Martin Phipps

Physics Department, McGill University, 3600 University Street, Montreal, Quebec, Canada H3A 2T8

Howard D. Trottier

** TRIUMF, 4004 Wesbrook Mall, Vancouver, British Columbia, Canada V6T 2A3*

(Received 22 October 1992)

We analyze the electromagnetic amplitude for the leptonic decays of pseudoscalar mesons in the quark model, with particular emphasis on $\eta \rightarrow l^+l^-$ ($l = e, \mu$). We evaluate the electromagnetic box diagram for a quark-antiquark pair with an arbitrary distribution of relative three-momentum \mathbf{p} : the amplitude is obtained to *all orders* in \mathbf{p}/m_q , where m_q is the quark mass. We compute $B_P \equiv \Gamma(\eta \rightarrow l^+l^-)/\Gamma(\eta \rightarrow \gamma\gamma)$ using a harmonic oscillator wave function that is widely used in nonrelativistic (NR) quark model calculations, and with a relativistic momentum space wave function that we derive from the MIT bag model. We also consider a quark model calculation in the limit of extreme NR binding due to Bergström. Numerical calculations of B_P using these three parametrizations of the wave function agree to within a few percent over a wide kinematical range. Our results show that the quark model leads in a natural way to a negligible value for the ratio of dispersive to absorptive parts of the electromagnetic amplitude for $\eta \rightarrow \mu^+\mu^-$ (unitary bound). However we find substantial deviations from the unitary bound in other kinematical regions, such as $\eta, \pi^0 \rightarrow e^+e^-$. Using the experimental branching ratio for $\eta \rightarrow \gamma\gamma$ as input, these quark models yield $B(\eta \rightarrow \mu^+\mu^-) \approx 4.3 \times 10^{-6}$, within errors of the recent SATURNE measurement of $5.1 \pm 0.8 \times 10^{-6}$, and $B(\eta \rightarrow e^+e^-) \approx 6.3 \times 10^{-9}$. While an application of constituent quark models to the pion should be viewed with particular caution, the branching ratio $B(\pi^0 \rightarrow e^+e^-) \approx 1.0 \times 10^{-7}$ is independent of the details of the above quark model wave functions to within a few percent.

PACS number(s): 13.40.Hq; 12.40.Qq; 13.20.Jf; 14.40.Aq

I. INTRODUCTION

The rare leptonic decays of pseudoscalar mesons, such as $\pi^0 \rightarrow e^+e^-$ and $\eta, K \rightarrow l^+l^-$ ($l = e, \mu$), provide sensitive probes of new physics both in and beyond the standard model [1]. In the case of the π^0 and η decays, a careful analysis of the electromagnetic contribution to the amplitude is required in order to isolate a possible contribution from new physics. While the absorptive part of the electromagnetic amplitude can be reliably determined by unitarity from experimental data on the two-photon width of the pseudoscalar, theoretical estimates of the dispersive part are in some disagreement [2].

An improved experimental measurement of the branching ratio for $\eta \rightarrow \mu^+\mu^-$ has recently been obtained at the η meson facility SATURNE in Saclay [3], with the result $B(\eta \rightarrow \mu^+\mu^-) = 5.1 \pm 0.8 \times 10^{-6}$. This is to be compared with the lower limit obtained by neglecting the dispersive part of the electromagnetic amplitude, yield-

ing the so-called unitary bound $B(\eta \rightarrow \mu^+\mu^-) \geq B^{\text{unit}} = 4.3 \times 10^{-6}$.

The SATURNE measurement is significantly closer to the unitary limit than previous experiments (for a compilation of earlier measurements see Ref. [4]). It is therefore of interest to reconsider the theoretical situation with respect to the magnitude of the dispersive contribution to the electromagnetic amplitude in this general class of decays.

The unitary bound for the leptonic decay of a pseudoscalar meson \mathcal{P} is most conveniently expressed in terms of the ratio of leptonic to two-photon widths

$$B_P \equiv \frac{\Gamma(\mathcal{P} \rightarrow l^+l^-)}{\Gamma(\mathcal{P} \rightarrow \gamma\gamma)} \equiv \frac{1}{2} \left(\frac{\alpha m_l}{\pi m_P} \right)^2 v |R|^2, \quad (1)$$

where m_P is the meson mass, and v is the lepton velocity in the center of mass:

$$v = \sqrt{1 - 4 \frac{m_l^2}{m_P^2}}. \quad (2)$$

To establish our notation, we express R in terms of a ratio of the amplitudes for the two modes. The invariant

*Present address: Department of Physics, Simon Fraser University, Burnaby, B.C., Canada V5A 1S6.

amplitude for the leptonic decay can be parametrized as

$$\mathcal{M}(\mathcal{P} \rightarrow l^+ l^-) \equiv \frac{e^4}{16\pi^2} m_l \bar{u}(\bar{k}) \gamma^5 v(k) L, \quad (3)$$

where the explicit factor of the lepton mass m_l reflects the helicity flip that occurs over the lepton line in Fig. 1. The width is given by

$$\Gamma(\mathcal{P} \rightarrow l^+ l^-) = \frac{\alpha^4}{8\pi} m_l^2 m_{\mathcal{P}} v |L|^2. \quad (4)$$

The amplitude for the two-photon decay takes the form

$$\mathcal{M}(\mathcal{P} \rightarrow \gamma\gamma) \equiv i e^2 \epsilon_{\mu\nu\alpha\beta} \epsilon_1^\mu \epsilon_2^\nu q_1^\alpha q_2^\beta F, \quad (5)$$

where $\epsilon_{1,2}$ and $q_{1,2}$ are the polarizations and momenta of the two photons. The form factor F is purely real for the decay to on-shell photons. The width is

$$\Gamma(\mathcal{P} \rightarrow \gamma\gamma) = \frac{\alpha^2}{4} \pi m_{\mathcal{P}}^3 F^2, \quad (6)$$

and the form factor R for the relative branching ratio $B_{\mathcal{P}}$ of Eq. (1) follows

$$R \equiv \frac{L}{F}. \quad (7)$$

Unitarity implies a connection between $\text{Im} L$ and F , resulting in the following model-independent result for the absorptive part of R [5]

$$\text{Im} R = \frac{\pi}{v} \ln \left(\frac{1-v}{1+v} \right). \quad (8)$$

The unitary bound on $B_{\mathcal{P}}$ is obtained by assuming that the dispersive part of R is negligible. In the case of $\eta \rightarrow \mu^+ \mu^-$, Eq. (8) implies $B_{\mathcal{P}} \geq B_{\mathcal{P}}^{\text{unit}} = 1.1 \times 10^{-5}$. When combined with the experimental result for the two-photon branching ratio (Ref. [4]), this leads to the unitary limit for $B(\eta \rightarrow \mu^+ \mu^-)$ quoted above. In general, a nonvanishing dispersive part leads to a correction to the unitary bound given by

$$\frac{B_{\mathcal{P}}}{B_{\mathcal{P}}^{\text{unit}}} = 1 + \left(\frac{\text{Re} R}{\text{Im} R} \right)^2. \quad (9)$$

Most theoretical calculations of the dispersive part of R have been based on a pointlike coupling of the pseudoscalar to off-shell photons [6], including dispersion re-

lations and vector meson dominance. Alternatively, a pointlike coupling of the pseudoscalar to nucleons or quarks (which then decay to virtual photons through a triangle diagram) has also been considered [7]. Recently, a calculation of η and π meson leptonic decays has been made in chiral perturbation theory [8].

We consider instead a bound-state description of the quarks which comprise the meson. We evaluate the leptonic decay $\mathcal{P} \rightarrow l^+ l^-$ at the quark level, which proceeds through the one-loop diagrams illustrated in Fig. 1. This approach was considered by Bergström [9] in the limit of extreme nonrelativistic binding, where the bound-state quarks are assumed to be at rest in the center of mass of the meson (and the meson mass is assumed to be exactly twice the quark rest mass). These approximations must be viewed with caution however when applied to light mesons such as the η .

In this paper we allow the quarks to have an arbitrary distribution of relative three-momentum \mathbf{p} . We compute the quark model amplitude for $\mathcal{P} \rightarrow l^+ l^-$ to *all orders* in \mathbf{p}/m_q , where m_q is the quark mass. A quark model wave function supplies the distribution of relative three-momenta for the quark-antiquark ($q\bar{q}$) bound state.

This approach is well known in nonrelativistic (NR) quark models [10–13], and has been used in a variety of applications, including calculations of the two-photon widths of light pseudoscalars [14, 12]. We make use of two parametrizations of the momentum space wave function: a harmonic oscillator form that is widely used in NR quark model calculations [12, 13], and a new relativistic parametrization that we derive from the MIT bag model. We also compare with the extreme nonrelativistic limit obtained by Bergström.

Although the NR quark model and the MIT bag model both give successful phenomenological descriptions of light hadrons, we use these models here mainly because they provide simple analytical expressions for the momentum space wave function in two limits that characterize a wide class of models. Our purpose in this paper is to make an estimate of momentum-dependent effects in the quark model amplitude for $\mathcal{P} \rightarrow l^+ l^-$, rather than to assess the predictive power of a particular model.

We expect that some of the model dependence inherent in a description of light quark binding may cancel in the relative branching fraction $B_{\mathcal{P}}$. In fact, our numerical calculations using the above parametrizations of the wave function agree to within a few percent over a wide kinematical range. Our results show that the quark model leads in a natural way to a negligible value for the ratio of dispersive to absorptive parts of the electromagnetic amplitude for $\eta \rightarrow \mu^+ \mu^-$. On the other hand, we find substantial deviations from the unitary bound in other kinematical regions, such as $\eta, \pi^0 \rightarrow e^+ e^-$.

The rest of this paper is organized as follows. In Sec. II, we describe our method for the evaluation of $\mathcal{P} \rightarrow l^+ l^-$ for a quark-antiquark pair with an arbitrary distribution of relative three-momentum. We evaluate the electromagnetic box diagram for the leptonic decay in closed form. In Sec. III, we present quantitative results using a harmonic oscillator wave function. In Sec. IV we derive a relativistic momentum space wave function based on the

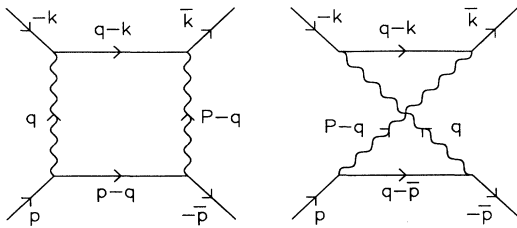


FIG. 1. Quark model electromagnetic box diagrams for $\mathcal{P} \rightarrow l^+ l^-$. In a “mock meson” description (Sec. II), the quark momenta in the center of mass are anticorrelated, $p, \bar{p} = (p^0, \pm \mathbf{p})$. The lepton momenta are $k, \bar{k} = (k^0, \pm \mathbf{k})$.

MIT bag model, which we also use to obtain quantitative results. We summarize our findings in Sec. V.

II. “MOCK MESON” METHOD

A. General framework

A conventional approach to the evaluation of hadronic matrix elements is to decompose the bound state into a superposition of free plane wave quark-antiquark ($q\bar{q}$) pairs [10–12]. An economical and physically reasonable description of the momentum space wave function is obtained by assuming that the quark and antiquark have equal and opposite three-momentum in each component of the plane wave expansion. In this “mock meson” description, the momentum space state vector $|M(P)\rangle$ for a meson in the center-of-mass frame [$P = (m_P, \mathbf{0})$] has the decomposition [12]

$$|M(P)\rangle \equiv \sqrt{2m_P} \int \frac{d^3\mathbf{p}}{(2\pi)^{3/2}} \Phi(\mathbf{p}) \frac{1}{2E_p} |q(\mathbf{p})\rangle |\bar{q}(-\mathbf{p})\rangle, \quad (10)$$

where $E_p \equiv \sqrt{\mathbf{p}^2 + m_q^2}$, and m_q is the quark mass. We have omitted color, spin, and flavor indices in Eq. (10) for convenience. We use invariant normalizations throughout this paper, e.g., $\langle q(\mathbf{p}') | q(\mathbf{p}) \rangle = 2E_p (2\pi)^3 \delta^3(\mathbf{p}' - \mathbf{p})$. The wave packet amplitude $\Phi(\mathbf{p})$ is normalized according to

$$\int d^3\mathbf{p} |\Phi(\mathbf{p})|^2 = 1. \quad (11)$$

For the ground-state pseudoscalar mesons of interest here, we assume that the wave function is spherically symmetric, $\Phi(\mathbf{p}) = \Phi(p)$.

The right-hand side of Eq. (10) is a (zero) momentum eigenstate, by construction. However, since the quarks are taken to be on shell, the energies of the individual $q\bar{q}$ plane wave components are in general not equal to the bound-state energy. This energy “mismatch” leads to several ambiguities in mock meson calculations, including the value to be used for the total $q\bar{q}$ energy running through intermediate states in the amplitude, and in phase space factors [12, 13]. A popular prescription is to identify the total $q\bar{q}$ energy appearing in the amplitude with the mean energy of the wave packet [12]. In the case of quark model calculations of the pseudoscalar two-photon width for example [12], this prescription leads to a phase space dependence on the meson mass that is in agreement with phenomenological estimates of the $\eta - \eta'$ mixing angle (see, e.g., Ref. [4]).

For the purpose of calculating the amplitude R however, it is crucial to take the total energy of the wave packet running through intermediate states to be equal to the physical meson mass (the relative branching fraction B_P is very insensitive to overall phase space factors, on the other hand). This is necessary in order to obtain the correct unitarity relation Eq. (8) between the absorptive part of the amplitude for the leptonic decay, and the (on-shell) two-photon matrix element. This prescription

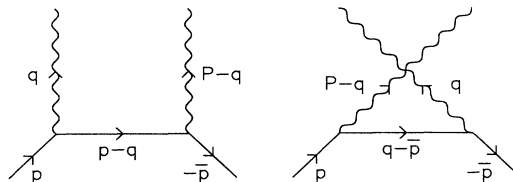


FIG. 2. Quark model diagrams for $\mathcal{P} \rightarrow \gamma\gamma$.

has also been used in other “mock meson” calculations [15].

In the extreme nonrelativistic limit Eq. (10) implies that the $q\bar{q}$ annihilation amplitude is proportional to the coordinate-space wave function (or its derivatives) at the origin [10, 11]. This limit has been used for example to make calculations of heavy quarkonium matrix elements [16], and was used by Bergström in a calculation of $\mathcal{P} \rightarrow l^+l^-$ [9].

Equation (10) has been used to *all orders* in the $q\bar{q}$ relative momentum in nonrelativistic quark model calculations of various matrix elements [12, 13], including pseudoscalar meson decay to two photons, Eq. (5). The form factor F is found by evaluation of the Feynman diagrams in Fig. 2 [14, 12]:

$$F = \frac{4\sqrt{3}}{\sqrt{2\pi}} \frac{m_q}{m_P^{3/2}} Q^2 \int p dp \Phi(p) \ln \left[\frac{E_p + p}{E_p - p} \right], \quad (12)$$

where the logarithm comes from an integration of the quark propagator over angles (assuming that the wave function Φ is spherically symmetric). Q is the quark charge in units of the proton charge. For decays of flavor-mixed states such as η , it is understood that an expectation value of the above expression for F is taken between the meson flavor wave function and the vacuum.

Equation (12) is obtained by assuming that each plane wave component of the $q\bar{q}$ wave packet has the same total energy [14, 12]. In our case, this means that a factor of $1/m_P$ is extracted from the quark propagator, which is contained in the overall factor of the meson mass in Eq. (12).

B. Application to leptonic decays

We derive the mock meson amplitude for $\mathcal{P} \rightarrow l^+l^-$ along the same lines which led to Eq. (12) for the two-photon matrix element:

$$\mathcal{M}(\mathcal{P} \rightarrow l^+l^-) = \sqrt{2m_P} \int \frac{d^3\mathbf{p}}{(2\pi)^{3/2}} \frac{1}{2E_p} \Phi(p) \mathcal{M}_{q\bar{q}}(\mathbf{p}), \quad (13)$$

where $\mathcal{M}_{q\bar{q}}$ is the amplitude for a given three-momentum component of the $q\bar{q}$ wave packet,

$$\mathcal{M}_{q\bar{q}}(\mathbf{p}) = -i2\sqrt{3}e^4Q^2 \int \frac{d^4q}{(2\pi)^4} Q^{\mu\nu}(q) L_{\mu\nu}(q) \frac{1}{[q^2 + i\epsilon][(P-q)^2 + i\epsilon][(p-q)^2 - m_q^2 + i\epsilon][(q-k)^2 - m_l^2 + i\epsilon]}. \quad (14)$$

The factor of 2 above accounts for the equal contribution of the two diagrams in Fig. 1, and $\sqrt{3}$ is a color factor. $Q^{\mu\nu}$ is the spin-singlet $q\bar{q}$ current:

$$Q^{\mu\nu} \equiv \frac{1}{\sqrt{2}} \sum_{\lambda=\pm} \lambda \bar{v}_{-\lambda}(-\mathbf{p}) \gamma^\nu [\not{p} - \not{q} + m_q] \gamma^\mu u_\lambda(\mathbf{p}) = \frac{4i}{\sqrt{2}} m_q \epsilon^{0\alpha\mu\nu} q_\alpha, \quad (15)$$

where, e.g., $u_\lambda(\mathbf{p})$ is a positive energy spinor of three-momentum \mathbf{p} and angular momentum $\lambda/2$ along a fixed quantization axis. $L^{\mu\nu}$ is the spin-singlet projection of the lepton current

$$L^{\mu\nu} = 2i \frac{m_l}{m_P} \epsilon^{0\alpha\mu\nu} q_\alpha \bar{u}(\bar{k}) \gamma^5 v(k) \quad (16)$$

[spin-triplet components of $L^{\mu\nu}$ vanish under contraction with $Q^{\mu\nu}$, or under integration in Eq. (13)].

Comparison of Eqs. (13)–(16) with Eq. (3) yields the following expression¹ for the form factor L :

$$L = 16\sqrt{3} \frac{m_q}{\sqrt{m_P}} Q^2 \int \frac{d^3\mathbf{p}}{(2\pi)^{3/2}} \Phi(p) \frac{1}{E_p} I(\mathbf{p}), \quad (17)$$

where

$$I(\mathbf{p}) = \frac{1}{i\pi^2} \int d^4q \frac{-\mathbf{q}^2}{[q^2 + i\epsilon][(P-q)^2 + i\epsilon][(p-q)^2 - m_q^2 + i\epsilon][(q-k)^2 - m_l^2 + i\epsilon]}. \quad (18)$$

This integral can be evaluated analytically. An identity relating \mathbf{q}^2 to a linear combination of (inverse) propagators reduces the integral to a sum of scalar three- and four-point functions, plus an integral of three propagators with a factor of q^0 in the numerator. A fictitious photon mass is introduced in intermediate calculations as the scalar vertex and box functions obtained in this way are infrared divergent (the total integral is infrared finite). We evaluate the divergent integrals using the expressions provided in Ref. [17]. After some algebra, we find

$$I(\mathbf{p}) = \frac{1}{4\sqrt{(p \cdot k)^2 - m_q^2 m_l^2}} \left[\ln(x_p) I_L + I_R \right], \quad (19)$$

where

$$I_L \equiv 2 + \ln\left(\frac{m_q m_l}{m_P^2}\right) + 2 \ln(1 - x_p^2) - \frac{1}{2} \ln(x_p) + i\pi, \quad (20)$$

$$I_R \equiv -\frac{\pi^2}{6} + \frac{1}{2} \ln^2\left(\frac{m_l}{m_q}\right) + \text{Sp}(x_p^2) + \text{Sp}\left(1 - x_p \frac{m_l}{m_q}\right) + \text{Sp}\left(1 - x_p \frac{m_q}{m_l}\right), \quad (21)$$

and

$$x_p \equiv \frac{p \cdot k - \sqrt{(p \cdot k)^2 - m_q^2 m_l^2}}{m_q m_l}. \quad (22)$$

$\text{Sp}(x)$ is the Spence function:

$$\text{Sp}(x) = - \int_0^x dt \frac{\ln(1-t)}{t}. \quad (23)$$

A crucial intermediate step in our evaluation of the loop integral in Eq. (18) is the identification of the total energy of each component of the $q\bar{q}$ wave packet with the physical meson mass (i.e., $P^0 \equiv m_P$). This is necessary in order to satisfy the unitarity relation of Eq. (8). In particular, without this prescription for the wave packet energy, the loop integral would acquire unphysical branch cuts that do not correspond to the ‘‘unitarity cut’’ through the intermediate photons in Fig. 1. On the other hand, we do use the actual plane wave energy $p^0 = E_p = \sqrt{\mathbf{p}^2 + m_q^2}$ in our final expression Eq. (19) for $I(\mathbf{p})$. We note that a similar prescription has been used in other mock meson calculations, such as the two-photon width [cf. Eq. (12) and Refs. [14, 12]].

The fact that our final expression for $\text{Im } L$ exactly satisfies the unitarity relation of Eq. (8) is a nontrivial check of the above prescription for handling the ambiguity in the wave packet energy. Indeed, after an analytical evalu-

¹As with Eq. (12) for the on-shell two-photon form factor, it is understood that an expectation value of Eq. (17) for L is taken in the case of a flavor-mixed state.

ation of the angular integration over $\text{Im} I(\mathbf{p})$ [Eqs. (17), (19), and (20)], we find that $\text{Im} L$ can be written as a product of Eq. (12) for the on-shell two-photon form factor F , times the right-hand side of Eq. (8).

III. HARMONIC OSCILLATOR WAVE FUNCTION

We evaluate the quark model form factor R [Eqs. (1), (7), (8), (12), and (17)] using a harmonic oscillator parametrization of the $q\bar{q}$ momentum space wave function that has been widely used in nonrelativistic quark model calculations [12, 13]:

$$\Phi_{\text{osc}}(\mathbf{p}) \equiv (\beta^2\pi)^{-3/4} \exp\left(-\frac{\mathbf{p}^2}{2\beta^2}\right). \quad (24)$$

Some representative results for the ratio $\text{Re} R/\text{Im} R$ obtained with this wave function are given in Fig. 3. For the sake of illustration, in this figure we take the ‘‘physical’’ mass of the hypothetical meson to be equal to the mean energy of the wave packet ($m_P = 2\langle E_p \rangle$).

In the limit $\beta/m_q \rightarrow 0$, the wave packet becomes nonrelativistic, with $\langle E_p \rangle \rightarrow m_q$. Bergström has made a quark model calculation of R in the extreme nonrelativistic (ENR) limit, taking the quark and antiquark to be at rest in the center of mass of the meson, with $2m_q \equiv m_P$ [9]. He found

$$\text{Re}(R_{\text{ENR}}) = \frac{2}{v} \left\{ \frac{1}{4} \ln^2\left(\frac{1+v}{1-v}\right) - \ln\left(\frac{1+v}{1-v}\right) + \frac{\pi^2}{12} + \text{Sp}\left(-\frac{1-v}{1+v}\right) \right\}. \quad (25)$$

Our results agree with Eq. (25) in the limit $\beta/m_q \rightarrow 0$.

We see that the real part of R is generally small compared to its imaginary part, except for small lepton masses $m_l \ll m_P$, or in the limit of ultrarelativistic binding $m_q \ll m_P$ ($\text{Re} R$ exhibits a logarithmic divergence as

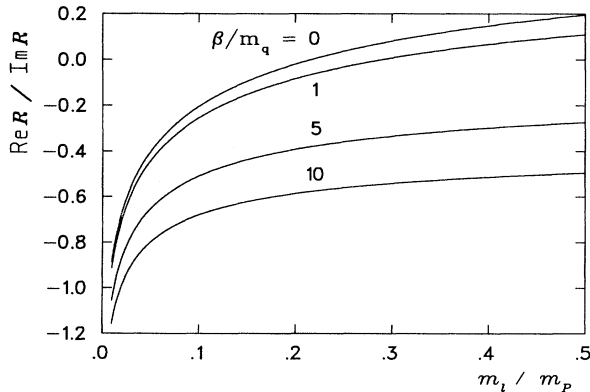


FIG. 3. Real part of the form factor R for the relative branching fraction $B_P(\mathcal{P} \rightarrow l^+l^-)$, compared to the unitarity result for the imaginary part [cf. Eqs. (1) and (8)], in a harmonic oscillator model of the bound-state wave function [Eq. (24)]. For this figure, the mass of the hypothetical meson is set equal to the mean energy of the $q\bar{q}$ wave packet.

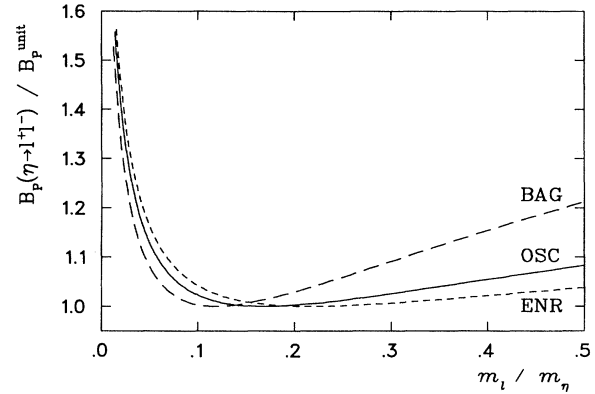


FIG. 4. Relative branching fraction B_P for the leptonic decay of the physical η meson, compared to the unitary bound B_P^{unit} . The three curves correspond a harmonic oscillator model [Eqs. (24) and (26)], a bag-model-inspired relativistic wave function [Eqs. (32) and (33)], and the limit of extreme nonrelativistic binding [Eq. (25)].

m_l or m_q go to zero, which is characteristic of mass singularities in loop processes).² Since the dispersive part of R appears quadratically in the branching ratio, we can expect small corrections to the unitary limit over a wide kinematical range.

To make contact with experimental data on $\eta \rightarrow l^+l^-$, we assign physical values to the quark model parameters and meson mass. Various sets of values for the quark masses and the wave-function Gaussian parameter β have been used in the literature [12, 13]. Our results for the relative branching fraction B_P are insensitive to variations in these parameters over a wide range.³ We use the typical values [18]

$$\begin{aligned} m_u = m_d &= 330 \text{ MeV}, \\ m_s &= 550 \text{ MeV}, \\ \beta &= 310 \text{ MeV}, \end{aligned} \quad (26)$$

and an η - η' mixing angle of -20° (cf. Ref. [4]).

We plot the relative branching fraction B_P compared to the unitary bound B_P^{unit} [Eq. (9)] in Fig. 4, for a range of lepton masses. We take m_P equal to the physical η mass when evaluating Eqs. (12) and (17). We also

²We include curves in Fig. 3 to illustrate the results of a harmonic oscillator calculation in the ultrarelativistic region; however, the physical region in this model corresponds to β/m_q of order unity or smaller.

³The absolute normalizations of the individual widths $\Gamma(\mathcal{P} \rightarrow \gamma\gamma)$ and $\Gamma(\mathcal{P} \rightarrow \mu^+\mu^-)$ depend strongly on the choice of model parameters. The widths also depend on the choice of total $q\bar{q}$ energy that is used in the phase space [12, 13]. The oscillator wave-function results for the two-photon widths of π^0 , η , and η' are generally within a factor of a few of the experimental values [12].

include a plot of B_P as obtained by Bergström in the limit of extreme nonrelativistic binding [cf. Eq. (25) and Ref. [9]]. The harmonic oscillator and ENR results differ by less than 5% over the entire kinematical region in m_l/m_η .

Using the experimental value for the two-photon branching fraction as input [4], we find $B(\eta \rightarrow \mu^+ \mu^-) = 4.3 \times 10^{-6}$ and $B(\eta \rightarrow e^+ e^-) = 6.3 \times 10^{-9}$ in the harmonic oscillator model. The result for the decay to muons is within errors of the recent SATURNE measurement $B_{\text{expt}}(\eta \rightarrow \mu^+ \mu^-) = 5.1 \pm 0.8 \times 10^{-6}$ [3], and is only 0.2% larger than the unitary limit. On the other hand, the branching fraction to electrons is ≈ 3.6 times larger than the corresponding unitary limit. We also compute $B(\pi^0 \rightarrow e^+ e^-) = 1.0 \times 10^{-7}$ in the oscillator model (about twice the unitary limit), although an application of constituent quark models to the pion should be viewed with particular caution.

IV. BAG-MODEL-INSPIRED RELATIVISTIC WAVE FUNCTION

Although the mock meson method described in Sec. II A was developed in the context of nonrelativistic quark models [12, 13], we find that the MIT bag model [19] can be used to motivate a relativistic parametrization of Eq. (10). We note in this connection that the momentum space wave packet distribution $\Phi(\mathbf{p})$ is, in principle, an arbitrary function, and need not be localized around momenta that are small compared to the quark mass [12].

To begin with, we must take account of the fact that bound states in the usual bag model are not momen-

tum eigenstates, while the quark and antiquark in Eq. (10) for the mock meson have equal and opposite three-momentum by construction. Our approach is complementary to the formalism introduced by Donoghue and Johnson, who introduced a wave packet in order to decompose the bag model wave function into momentum eigenstates [20]. Their wave packet is determined by normalizing to a particular matrix element, such as f_π . We choose instead to identify the wave packet amplitude $\Phi(\mathbf{p})$ in Eq. (10) directly from the Fourier transform of the cavity wave function.

To begin with, consider the wave function for the ground state of a single quark in a cavity of radius R :

$$\psi_\lambda(\mathbf{r}) = \mathcal{N} \begin{bmatrix} \left(\frac{\omega_0 + m_0}{\omega_0}\right)^{1/2} i j_0\left(\frac{xr}{R}\right) U_\lambda \\ - \left(\frac{\omega_0 - m_0}{\omega_0}\right)^{1/2} j_1\left(\frac{xr}{R}\right) \boldsymbol{\sigma} \cdot \hat{\mathbf{r}} U_\lambda \end{bmatrix} \quad (r \leq R), \quad (27)$$

where for later use we label the ‘‘current’’ quark mass by m_0 , and where $\omega_0 \equiv (x^2/R^2 + m_0^2)^{1/2}$. The momentum eigenvalue x is determined by the boundary condition $\tilde{\psi}\psi|_{r=R} = 0$ [19]. \mathcal{N} is a normalization, and U_λ is a two-component spinor with polarization $\lambda = \pm$ along the z axis.

The Fourier transform of a Dirac wave function can be found by standard methods [21]. Since we can decompose the wave function along an arbitrary complete set of states, the plane wave spinors in the Fourier transform of Eq. (27) need not have the same (‘‘current’’) quark mass m_0 as $\psi_\lambda(\mathbf{r})$. We compute a Fourier transform along plane waves of arbitrary ‘‘effective’’ mass m_{eff} :

$$\psi_\lambda(\mathbf{r}) = \int \frac{d^3\mathbf{p}}{(2\pi)^{3/2}} \frac{1}{\sqrt{2\omega_{\text{eff}}(p)}} \left[\phi(p) u_\lambda(\mathbf{p}) e^{i\mathbf{p}\cdot\mathbf{r}} + \tilde{\phi}(p) \sum_{\lambda'=\pm} S_{\lambda\lambda'}(\hat{\mathbf{p}}) v_{\lambda'}(\mathbf{p}) e^{-i\mathbf{p}\cdot\mathbf{r}} \right], \quad (28)$$

where $u_\lambda(\mathbf{p})$ and $v_\lambda(\mathbf{p})$ are plane wave Dirac spinors with angular momentum $\lambda/2$ along the z axis, and $S_{\lambda\lambda'}(\hat{\mathbf{p}}) \equiv U_\lambda^\dagger \boldsymbol{\sigma} \cdot \hat{\mathbf{p}} U_{\lambda'}$. The spinors are normalized to $u^\dagger u = -v^\dagger v = 2\omega_{\text{eff}}(p)$, where $\omega_{\text{eff}}^2(p) \equiv \mathbf{p}^2 + m_{\text{eff}}^2$ [22].

The Fourier amplitudes ϕ and $\tilde{\phi}$ depend on the magnitude of the three-momentum $p \equiv |\mathbf{p}|$. We find [23]

$$\begin{aligned} \phi(p) = & \frac{1}{\sqrt{2\pi}} [\psi^\dagger(0)\psi(0)]^{1/2} \frac{R^2}{px} \left(\frac{\omega_{\text{eff}}(p) + m_{\text{eff}}}{2\omega_{\text{eff}}(p)} \right)^{1/2} \\ & \times \left\{ j_0(pR - x) - j_0(pR + x) + \left(\frac{\omega_0 - m_0}{\omega_0 + m_0} \right)^{1/2} \frac{p}{\omega_{\text{eff}}(p) + m_{\text{eff}}} [j_0(pR + x) + j_0(pR - x) - 2j_0(pR)j_0(x)] \right\}, \end{aligned} \quad (29)$$

and

$$\begin{aligned} \tilde{\phi}(p) = & \frac{1}{\sqrt{2\pi}} [\psi^\dagger(0)\psi(0)]^{1/2} \frac{R^2}{px} \left(\frac{\omega_{\text{eff}}(p) + m_{\text{eff}}}{2\omega_{\text{eff}}(p)} \right)^{1/2} \\ & \times \left\{ -\frac{p}{\omega_{\text{eff}}(p) + m_{\text{eff}}} [j_0(pR - x) - j_0(pR + x)] + \left(\frac{\omega_0 - m_0}{\omega_0 + m_0} \right)^{1/2} [j_0(pR + x) + j_0(pR - x) - 2j_0(pR)j_0(x)] \right\}. \end{aligned} \quad (30)$$

The usual mock meson approach to the calculation of hadronic matrix elements assumes that the quarks propagate as free particles in intermediate states [12]. For example, the explicit factor of the quark mass in the matrix

elements for $\mathcal{P} \rightarrow \gamma\gamma, l^+ l^-$ [Eqs. (12) and (17)] is due to the helicity flip along an intermediate quark line. In typical nonrelativistic quark model calculations, the quarks have large ‘‘constituent’’ masses. This means, for exam-

ple, that the u , d , and s quark components of the η and η' flavor wave functions make comparable contributions to their matrix elements in these models, in agreement with simple phenomenological estimates of the pseudoscalar mixing angle (see, e.g., Ref. [4]).

In typical MIT bag-model calculations however the quarks are assigned current masses, in particular, $m_{u,d} \approx 0$. In order to obtain a sensible phenomenological description of helicity-flip amplitudes in a mock meson approach, we must assume that a cavity quark propagates with a mass that is different from its “bare” value m_0 . We therefore assign a constituent (or effective) quark mass to intermediate quark lines, and for consistency we use the same effective mass in the Fourier transform Eq. (28) of the cavity wave function.

A rigorous calculation of matrix elements in the context of the bag model would use a cavity propagator for intermediate quark lines [24]. This was in fact done in a calculation of $\pi^0 \rightarrow \gamma\gamma$ in Ref. [25]. We note that the cavity quark propagator differs from the free propagator by some terms that act, to some extent, like a (momentum-dependent) effective mass. A calculation of the leptonic decay using cavity propagators would be quite involved however. On the other hand, our extension of the mock meson method to the bag model permits a straightforward evaluation of the matrix element incorporating much of the basic physics underlying cavity perturbation theory [this is further illustrated by our comments below Eq. (32)].

Although the actual value of the effective mass for “free” quark propagators is somewhat *ad hoc*, this approach can nevertheless be used with justification in the calculation of the form factor R of interest in this paper [Eq. (1)]. This is due to the fact that the *ratio* between the leptonic and two-photon amplitudes is insensitive to variations in the actual value of the effective quark mass over a large range. Observe in particular that the same factor of the intermediate quark mass due to the helicity flip appears in both matrix elements [cf. Eqs. (12) and (17)]. On physical grounds, the effective quark mass should be on the order of the cavity energy ω_0 ; we find that B_P changes by only a few percent as m_{eff} is varied from $\frac{1}{4}\omega_0$ to ω_0 . We use $m_{\text{eff}} = \omega_0$ in the following calculations.

At any rate, we do not regard our results as providing precise tests of the predictive power of the bag model. Our interest in this paper is to make an estimate of momentum-dependent effects in the correction to the unitary limit for $\mathcal{P} \rightarrow l^+l^-$ in the context of general quark models. In that respect, the bag-model-inspired wave packet amplitudes provide a very useful comparison with the harmonic oscillator wave function used in Sec. III. In particular, $\phi(p)$ falls off only as $1/p^2$ at large p , compared to the exponential decay of the oscillator wave function.

In this connection, we note that the mock meson wave packet of Eq. (10) is based on a single-particle description of the quark and the antiquark in the bound state, which is in general inadequate to describe localized relativistic states. This problem is shared by the single wave packet amplitude introduced by Donoghue and Johnson. A proper connection between the localized cavity wave

function and momentum space eigenstates requires the use of a Bogoliubov transformation [26], which in this case involves a mixing among the complete set of cavity eigenstates.

On the other hand, we find that the negative energy components of the Fourier transform actually make a small contribution to the normalization of the ground-state cavity mode. The cavity wave function Eq. (27) is normalized to one in the sphere of radius R , which implies

$$\int d^3\mathbf{p} \left(\phi^2(p) + \tilde{\phi}^2(p) \right) = 1. \quad (31)$$

We find that the contribution of the negative energy component to this normalization integral is at most 7% in the “ultrarelativistic” limit ($m_0R = 0$), and falls below 4% by $m_0R \sim 1$. We conclude that a reasonable approximation to the ground-state cavity wave function can be obtained by truncating the negative energy component of the Fourier transform in Eq. (28),⁴ and we therefore identify $\Phi(\mathbf{p})$ in the mock meson wave packet Eq. (10) as

$$\Phi_{\text{bag}}(\mathbf{p}) \equiv \phi(p) \quad (32)$$

[cf. Eqs. (11) and (31)].

We note that $\text{Re} R$ is very insensitive to the value of the current quark mass m_0 . This is due in large measure to the fact that we use an effective mass $m_{\text{eff}} = O(\omega_0)$ for intermediate quark propagators. Thus, even for a massless current quark, the effective mass is nonzero ($\omega_0R \in [2.04, \infty]$ for $m_0R \in [0, \infty]$). The logarithmic mass singularity that would be present in $\text{Re} R$ for a truly massless propagator is thereby avoided. A similar situation would occur in a rigorous calculation of the bag model width using cavity propagators.

We include our results for the relative branching fraction $B_P(\eta \rightarrow l^+l^-)$ for the physical η meson using this bag-model-inspired wave function in Fig. 4. We use the typical bag-model parameter values [19, 27]

$$\begin{aligned} m_u &= m_d = 0, \\ m_s &= 300 \text{ MeV}, \\ R &= 3.3 \text{ GeV}^{-1}. \end{aligned} \quad (33)$$

The results for B_P in the relativistic wave function agree with the harmonic oscillator calculation (and with the extreme nonrelativistic limit) to within a few percent over a wide range in m_l/m_η , except for large lepton masses, near threshold. This is evidently related to the fact that bag-model wave packet has appreciable components at large $q\bar{q}$ relative momentum [cf. $\Phi_{\text{bag}}(p) \sim 1/p^2$ at large p , compared to $\Phi_{\text{osc}}(p) \sim \exp(-p^2)$].

For the physical cases of η or π^0 decays to muons or electrons, m_l/m_P is small, and the bag-model-inspired

⁴Note that the normalization of the wave packet cancels in a calculation of the relative branching fraction B_P .

results $B(\eta \rightarrow \mu^+ \mu^-) = 4.4 \times 10^{-6}$, $B(\eta \rightarrow e^+ e^-) = 6.1 \times 10^{-9}$, and $B(\pi^0 \rightarrow e^+ e^-) = 1.0 \times 10^{-7}$ agree with the oscillator model to better than 5%.

V. SUMMARY

We have evaluated the electromagnetic box diagram for the leptonic decay of a pseudoscalar quark-antiquark pair with an arbitrary distribution of relative three-momentum. Quantitative results were obtained in three different models of the bound-state wave function (a non-relativistic harmonic oscillator model [12, 13], a new relativistic momentum space wave function that we derived from the MIT bag model, and in the limit of extreme non-relativistic binding, analyzed previously by Bergström [9]). Our results demonstrate that the relative branching fraction $B_P \equiv B(\mathcal{P} \rightarrow l^+ l^-) / B(\mathcal{P} \rightarrow \gamma\gamma)$ is insensitive to the details of the quark model wave function. In the case of η and π^0 decays, the results obtained with the harmonic oscillator and relativistic wave functions agree to within 5%.

We find that the quark model leads in a natural way to a negligible value for the ratio of dispersive to absorptive parts of the electromagnetic amplitude for $\eta \rightarrow \mu^+ \mu^-$. On the other hand, we find substantial deviations from

the unitary bound in other kinematical regions, such as $\eta \rightarrow e^+ e^-$.

Using the experimental branching ratio for $\eta \rightarrow \gamma\gamma$ as input, these quark models yield $B(\eta \rightarrow \mu^+ \mu^-) \approx 4.3 \times 10^{-6}$, within errors of the recent SATURNE measurement of $5.1 \pm 0.8 \times 10^{-6}$, and $B(\eta \rightarrow e^+ e^-) \approx 6.3 \times 10^{-9}$. While an application of constituent quark models to the pion should be viewed with particular caution, the quark models considered here yield $B(\pi^0 \rightarrow e^+ e^-) \approx 1.0 \times 10^{-7}$, independent of the details of the model wave function to within a few percent. This is to be compared with recent experimental data from Fermilab, $B_{\text{expt}}(\pi^0 \rightarrow e^+ e^-) = 6.9 \pm 2.8 \times 10^{-8}$ [28], and preliminary data from Brookhaven $B_{\text{expt}}(\pi^0 \rightarrow e^+ e^-) = 6.0 \pm 1.8 \times 10^{-8}$ [29]. The quark model branching ratios obtained here are comparable to the results of a recent analysis in chiral perturbation theory [8], which requires the experimental value of the branching ratio for $\eta \rightarrow \mu^+ \mu^-$ as input.

ACKNOWLEDGMENT

This work was supported in part by the Natural Sciences and Engineering Research Council of Canada.

-
- [1] For a recent topical review, see *Rare Decays of Light Mesons*, Proceedings of the International Workshop, Gif-sur-Yvette, France, 1990, edited by B. Mayer (Editions Frontières, Gif-sur-Yvette, France, 1990).
- [2] For reviews, see P. Herczeg, in *Rare Decays of Light Mesons* [1], p. 97; A. Soni, in *Proceedings of the Workshop on Physics with Light Mesons*, Los Alamos, New Mexico, 1987, edited by W. R. Gibbs and B. M. K. Nefkens (Los Alamos Report No. LA-11184-C, 1987), p. 55.
- [3] SATURNE Collaboration, M. Garçon *et al.*, Report No. DAPNIA/SphN 92 04 (unpublished).
- [4] Particle Data Group, K. Hikasa *et al.*, Phys. Rev. D **45**, S1 (1992).
- [5] S. M. Berman and D. A. Geffen, Nuovo Cimento **18**, 1192 (1960); D. A. Geffen and B.-L. Young, Phys. Rev. Lett. **15**, 316 (1965); C. G. Callan and S. B. Treiman, *ibid.* **18**, 1083 (1967); **19**, 57(E) (1967); C. Jarlskog and H. Pilkuhn, Nucl. Phys. **B1**, 264 (1967).
- [6] G. D. Ambrosio and D. Espriu, Phys. Lett. B **175**, 237 (1986); Ll. Ametller, A. Bramon, and E. Massó, Phys. Rev. D **30**, 251 (1984); L. Bergström and E. Ma, *ibid.* **29**, 1029 (1984); G. B. Tupper and M. A. Samuel, *ibid.* **26**, 3302 (1982); **29**, 1031 (1984); M. D. Scadron and M. Visinescu, *ibid.* **29**, 911 (1984); K. S. Babu and E. Ma, Phys. Lett. **119B**, 449 (1982).
- [7] M. Pratap and J. Smith, Phys. Rev. D **5**, 2020 (1972); Ll. Ametller, L. Bergström, A. Bramon, and E. Massó, Nucl. Phys. **B228**, 301 (1983).
- [8] M. J. Savage, M. Luke, and M. B. Wise, Phys. Lett. B **291**, 481 (1992).
- [9] L. Bergström, Z. Phys. C **14**, 129 (1982).
- [10] R. Van Royen and V. F. Weisskopf, Nuovo Cimento **50A**, 617 (1967).
- [11] J. M. Jauch and F. Rohrlich, *The Theory of Photons and Electrons* (Springer, New York, 1976).
- [12] C. Hayne and N. Isgur, Phys. Rev. D **25**, 1944 (1982).
- [13] Some applications of the mock meson method in the non-relativistic quark model can be found in S. Godfrey and N. Isgur, Phys. Rev. D **32**, 189 (1985); S. Godfrey, *ibid.* **33**, 1391 (1986); N. Isgur, B. Grinstein, and M. B. Wise, *ibid.* **39**, 799 (1989); S. Capstick and S. Godfrey, *ibid.* **41**, 2856 (1990); Z. P. Li, F. E. Close, and T. Barnes, *ibid.* **43**, 2161 (1991); P. J. O'Donnell and H. K. K. Tung, *ibid.* **44**, 741 (1991).
- [14] L. Bergström, H. Snellman, and G. Tengstrand, Phys. Lett. **82B**, 419 (1979).
- [15] See, for example, S. Capstick and S. Godfrey, Phys. Rev. D **41**, 2856 (1990).
- [16] For reviews, see T. Appelquist, R. M. Barnett, and K. Lane, Annu. Rev. Nucl. Part. Sci. **28**, 387 (1978); W. Kwong, J. L. Rosner, and C. Quigg, *ibid.* **37**, 325 (1987).
- [17] W. Beenakker and A. Denner, Nucl. Phys. **B338**, 349 (1990).
- [18] N. Isgur, B. Grinstein, and M. B. Wise, Phys. Rev. D **39**, 799 (1989).
- [19] A. Chodos, R. L. Jaffe, K. Johnson, C. B. Thorn, and V. F. Weisskopf, Phys. Rev. D **9**, 3471 (1974); T. DeGrand, R. L. Jaffe, K. Johnson, and J. Kiskis, *ibid.* **12**, 2060 (1975).
- [20] J. F. Donoghue and K. Johnson, Phys. Rev. D **21**, 1975 (1980).
- [21] See, for example, J. D. Bjorken and S. D. Drell, *Relativistic Quantum Mechanics* (McGraw-Hill, New York, 1964).
- [22] We verify by numerical integration that the expectation value of the "current" quark Hamiltonian operator $\alpha \cdot (-i\nabla) + \beta m_0$ in the wave packet of Eq. (28) is equal to

- the cavity eigenfrequency ω_0 for arbitrary effective quark mass m_{eff} .
- [23] Equation (29) for the positive energy component $\phi(p)$ of the Fourier transform was obtained by B. Margolis and R. R. Mendel, Phys. Rev. D **28**, 468 (1983), for the special case $m_{\text{eff}} = m_0$. However, the negative energy component $\tilde{\phi}(p)$ of the Fourier transform Eq. (28) was overlooked in the above paper.
- [24] T. H. Hansson and R. L. Jaffe, Phys. Rev. D **28**, 882 (1983).
- [25] B. A. Li, Phys. Lett. **134B**, 120 (1984); **151B**, 473(E) (1985).
- [26] N. N. Bogoliubov, Nuovo Cimento **7**, 794 (1958); J. Valatin, *ibid.* **7**, 843 (1958). See also W. A. Bardeen *et al.*, Phys. Rev. D **11**, 1094 (1976).
- [27] The η - η' mass splitting due to the $O(\alpha_s^2)$ gluon box diagram was computed in cavity perturbation theory with the bag-model parameters of Eq. (33) in J. G. Donoghue and H. Gomm, Phys. Rev. D **28**, 2800 (1983). See also K. Geiger, B. Müller, and W. Greiner, Z. Phys. C **48**, 257 (1990), for an analysis of η meson phenomenology in the bag model.
- [28] Fermilab experiment E799, in *Proceedings of the XXVIth International Conference on High Energy Physics*, Dallas, Texas, 1992, edited by J. Sanford (AIP, New York, 1993).
- [29] Brookhaven experiment E777 (unpublished).